

# Kinetics of Ion Formation in Rubidium Vapour Excited by

## Nanosecond Resonant Laser Pulses

M.A.Mahmoud<sup>1</sup> and Y.E.E.Gamal<sup>2</sup>

<sup>1</sup>*Department of Physics, Faculty of Science, Sohag University, Sohag 82524, Egypt*

<sup>2</sup>*National Institute of Laser Enhanced Science, Cairo University, El Giza, Egypt*

Abstract: We have studied theoretically formation of molecular ion  $\text{Rb}_2^+$  and the atomic ion  $\text{Rb}^+$  which are created in laser excited rubidium vapor at the  $5S_{1/2} \rightarrow 5P_{3/2}$  or  $5S_{1/2} \rightarrow 5P_{1/2}$  ( $\lambda_{D1}=780$  nm,  $\lambda_{D2}=795$  nm). A set of rate equations, which describe the temporal variation of the electron energy distribution function (EEDF), the electron density, the population density of the excited states as well as the atomic  $\text{Rb}^+$  and molecular ion  $\text{Rb}_2^+$ , are solved numerically. The calculations are carried out at different laser energy and different rubidium atomic vapor densities. The numerical calculations show that competition between associative ionization (5p-5p), and Molnar – Hornbeck ionization processes for producing  $\text{Rb}_2^+$ , the calculations have also shown that the atomic ions  $\text{Rb}^+$  are formed through the Penning ionization and photoionization processes. Also, the obtained results showed reasonable agreement with the experimentally measured values of the ion density given by Bakhramov et al [10].

### 1. Introduction

Laser –induced collisional ionization and plasma generation in gases by intense laser pulses have been extensively studied ever since high –intensity pulsed lasers have been developed. In applied science, the laser-plasma mechanism is important in various studies like laser fusion, energy conversion, optical switching [1], and others, while in pure science, laser breakdown is involved in studies like ion spectroscopy [2]. In low-temperature plasma physics, collisional ionization a well –known optical phenomenon. The efficiency of this process can be increased by many orders of magnitude when the laser wavelength corresponds to an absorption line of the ionized medium. Lucatorto and McIlrath [3] first observed this effect in sodium vapor with the laser pulses tuned to the first resonance line 3s-3p at  $\lambda=5890$  Å. Since then, efficient ionization by resonance radiation has been observed in all alkali – metal and alkaline –earth metal vapors tested rubidium [4-6], lithium [7,8] and barium [9]. In recent years, there has been an increased interest in the study of the collisional ionization and excitation energy transfer processes in a laser excited alkali vapor because of the importance of these processes in radiative transfers involved in gas lasers, astrophysics and controlled thermonuclear plasma [1,3]. On the other hand resonant laser excitation has played a vital role in coupling energy into vapor. Therefore the reaction of a dense rubidium vapour, resonantly irradiated by nanosecond pulsed laser, has been the subject of a number of investigations during the past few years [10-12]. These studies have shown that a large

variety of mechanisms take place in the excited media. Of particular interests are the ionization mechanisms and energy transfer mechanisms. Therefore, the present work aimed to investigate the actual contribution of each of these processes to the plasma generation in laser saturation of rubidium vapor. In doing so a numerical model is applied which includes photo ionization and collisional ionization of the saturated excited atoms, as electron seeding processes. In addition the model includes also electron impact and atom-atom collisional processes which leads eventually to plasma formation.

### 2. Rate equations

Calculations are based on a previously developed [11-12] numerical model which involves a system of rate equations that describe the variation of the population of the considered nineteen level ( $5d \leq nl \leq 11s$ ) of the rubidium atom in addition to atomic ion and molecular ion levels. In the present work the model is modified to take into account the pulsed nature of the laser beam. The model is applied to investigate the kinetics of ion formation in rubidium vapour under the experimental conditions given by Bakhramov et al [10]. In their experiment the rubidium vapor ( $10^{11} - 10^{14} \text{ cm}^{-3}$ ) was irradiated by resonance laser pulse of duration  $\approx 30$  ns (FWHM) and intensity varies between  $10 \text{ kWcm}^{-2} \leq I \leq 2 \text{ MWcm}^{-2}$  with line width  $\leq 0.25 \text{ cm}^{-1}$  which is tuned to the  $D_{1,2}$  –resonance line. The physical kinetic processes which are considered in our model and the values of the cross sections are indicated in table 1.

The equations describing the temporal variation of the population density of Rb levels 5s, 5p and nl were expressed in the form:

$$\frac{dN(5s)}{dt} = N(5p)(R_{21} + A_{21}) - N(5s)R_{12} + N(5p) \int n_e(\varepsilon)K_{21}(\varepsilon)d\varepsilon - N(5s) \int n_e(\varepsilon)K_{12}(\varepsilon)d\varepsilon + N(5p)N(n)K_{PI} + \frac{1}{2}N^2(5p)\sigma_{PL}vF + \frac{1}{2}N^2(5p)K_{EP} - N(n)N(5s)K_{HMI} - N(5s) \int n_e(\varepsilon)K_{1c}(\varepsilon)d\varepsilon \quad (1)$$

$$\frac{dN(5p)}{dt} = N(5s)R_{12} - N(5p)(R_{21} + A_{21}) - N(5p) \int n_e(\varepsilon)K_{21}(\varepsilon)d\varepsilon + N(5s) \int n_e(\varepsilon)K_{12}(\varepsilon)d\varepsilon - \frac{1}{2}N^2(5p)K_{AI} - N(5p)N(n)K_{PI} - \frac{1}{2}N^2(5p)\sigma_{PL}vF - \frac{1}{2}N^2(5p)K_{EP} - N(5p)\sigma_{2c}^{(2)}F^2 - N(5s) \int n_e(\varepsilon)K_{2c}(\varepsilon)d\varepsilon \quad (2)$$

$$\frac{dN(n)}{dt} = \sum_{m>n} n_e(\varepsilon)N(n)K_{nm}(\varepsilon) - \sum_{m<n} n_e(\varepsilon)N(n)K_{mn}(\varepsilon) - \sum_{m=n} A_{nm}N(n) - \sum_n n_e(\varepsilon)N(n)K_{nc}(\varepsilon) - \sum_n N(5p)N(n)K_{PI} + \frac{1}{2}N^2(5p)K_{EP} - \sum_n N(n)N(5s)K_{HMI} - \sum_{n>2} N(n)\sigma_{nc}^{(1)}F + N_{Rb^+}n_e(\varepsilon) \sum_n [n_e(\varepsilon)K_{cn}(\varepsilon) + K_{RD}(\varepsilon)] \quad (3)$$

where  $R_{21}$  ( $\text{sec}^{-1}$ ) represents the stimulated emission rate coefficient for transition from level 2 to 1.

$$R_{21} \equiv B_{21} \int I(\nu) L_{21}(\nu) d\nu / 4\pi \cong (I(\nu)/h\nu)\sigma_{21}(\nu) \quad (4)$$

$I(\nu)$  is the spectral irradiance of the radiation field at frequency  $\nu$  appropriate to the  $2 \rightarrow 1$  transition,  $B_{21}$  represents Milne coefficient, and  $L_{21}(\nu)$  represents the corresponding line profile function for the transition.  $A_{21}$  is the resonance transition Einstein coefficient for spontaneous emission.

$N(5s), N(5p)$  and  $N(n)$  represents the population density of 5s, 5p and nl states respectively. While  $n_e(\varepsilon)$  represents the free electron density as a function of electron energy  $\varepsilon$ .  $K_{mn}$  ( $\text{cm}^3 \text{sec}^{-1}$ ) represents the electron - collision rate coefficient for the  $m \rightarrow n$  transition [13],  $K_{nc}$  ( $\text{cm}^3 \cdot \text{sec}^{-1}$ ) represents the electron collisional ionization rate coefficient for level n [14],  $K_{cn}$  ( $\text{cm}^6 \text{sec}^{-1}$ ) represents the three body recombination rate coefficient [14],  $K_{RD}$  ( $\text{cm}^3 \text{sec}^{-1}$ ) represents the irradiative recombination rate coefficient to level n [14].  $K_{AI} = \sigma_{AI} v$  and represent the rate coefficients of associative ionization.

$K_{HMI} = \sigma_{HMI} v$ , represent the rate coefficient Hornbeck- Molnar ionization.  $K_{PI} = \sigma_{PI} v$  represents the rate coefficients Penning ionization.  $K_{EP} = \sigma_{EP} v$  represents the rate coefficient of energy pooling collisions. Where  $\sigma_{AI}, \sigma_{HMI}, \sigma_{PI}$  and  $\sigma_{EP}$  are the cross sections of the associative ionization, Hornbeck-Molnar ionization, Penning ionization and energy pooling processes respectively.  $\sigma_{PL}$  is laser-assisted Penning ionization cross section,  $v$  is the average velocity of atoms.  $\sigma_{nc}^{(1)}$  is the single-photon ionization cross section for level n,  $\sigma_{2c}^{(2)}$  is the two

photon, resonance state ionization rate coefficient and  $F$  represents the photon flux density.

The time evolution of the electron density as a function of electron energy  $\varepsilon$  is given by,

$$\frac{dn_e(\varepsilon)}{dt} = \sum_{m>n} n_e N(m)K_{nm}(\varepsilon) - \sum_{m<n} n_e(\varepsilon)N(n)K_{mn}(\varepsilon) + \sum_n n_e(\varepsilon)N(n)K_{nc}(\varepsilon) + \sum_n N(5p)N(n)K_{PI} + N(5p)\sigma_{2c}^{(2)}F^2 + \sum_{n>2} N(n)\sigma_{nc}^{(1)}F + \frac{1}{2}N^2(5p)\sigma_{PL}vF + \frac{1}{2}N^2(5p)K_{AI} + \sum_n N(n)N(5s)K_{HMI} - N_{Rb^+}n_e(\varepsilon) \sum_n [n_e(\varepsilon)K_{cn}(\varepsilon) + K_{RD}(\varepsilon)] \quad (5)$$

The rate of growth of the molecular ion and the atomic ion is given by

$$\frac{dN(Rb_2^+)}{dt} = \frac{1}{2}N^2(5p)K_{AI} + N(n)N(5s)K_{HMI} \quad (6)$$

$$\frac{dN(Rb^+)}{dt} = \sum_n N(5p)N(n)K_{PI} + \sum_n n_e(\varepsilon)N(n)K_{nc}(\varepsilon) + N(5p)\sigma_{2c}^{(2)}F^2 + \sum_{n>2} N(n)\sigma_{nc}^{(1)}F + \frac{1}{2}N^2(5p)\sigma_{PL}vF - N(Rd^+)n_e(\varepsilon) \sum_n [n_e(\varepsilon)K_{cn}(\varepsilon) + K_{RD}(\varepsilon)] \quad (7)$$

Table.1. Values of Energy pooling, Associative ionization, Penning ionization and photon ionization processes cross sections in laser excited rubidium atoms.

Ionization process	nl	Cross section	Ref
Energy pooling collisions $\sigma_{EP} \times 10^{-14}$ ( $\text{cm}^2$ )	5d	3	5
Hornbeck-Molnar ionization $\sigma_{HMI} \times 10^{-15}$ ( $\text{cm}^2$ )	6d	3.4	6
	8s	4.7	6
	7d	4.9	6
Penning ionization $\sigma_{PI} \times 10^{-12}$ ( $\text{cm}^2$ )	5d	3.5	6
	6d	4.7	6
	8s	1.6	6
	7d	2.8	6
	8d	3.1	6
Associative ionization $\sigma_{AI} \times 10^{-16}$ ( $\text{cm}^2$ )	3/2	5.4	10
	1/2	0.14	
Two-photon ionization $\sigma^{(2)} 5P_{J \rightarrow c} \times 10^{-47}$ ( $\text{cm}^4 \cdot \text{sec}$ )	3/2	2.8	10
	1/2	0.3	10
Laser-assisted Penning ionization $\sigma_{PL} \times 10^{-41}$ ( $\text{cm}^4 \cdot \text{sec}$ )	3/2	4.5	10
	1/2	5.8	10
Single-photon ionization $\sigma^{(1)} \times 10^{-18}$ ( $\text{cm}^2$ )	6p	15	15
	5d	16	15
	7p	7.0	15
	6d	8.0	15
	8s	7.1	15
	7d	5.7	15

### 3. Results and discussions

The above shown set of equations (1-7) are solved numerically using the Rung-Kutta fourth-

order technique under the experimental conditions of Bakhrarov et al [10]. A computer program is under taken to obtain the following relations (i) The density of  $Rb_2^+$  and  $Rb^+$  as a function of the rubidium atomic density at different exposed times. (ii) The effect of laser power intensity on the rubidium ions generated during the interaction of rubidium vapour with laser radiation.

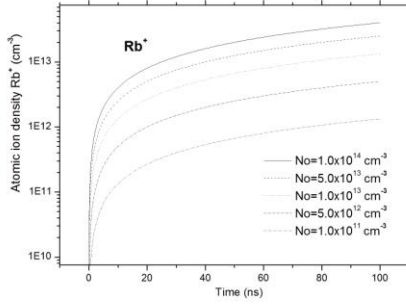
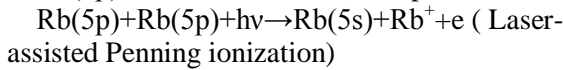


Figure.1. Time evolution of Atomic ion  $Rb^+$  at different rubidium vapour densities and laser power  $1 \times 10^5 \text{ W.cm}^{-2}$ .

### 3.1 The time evolution of the atomic ion $Rb^+$

The growth rate of the  $Rb^+$  as a function of time is indicated in Figure.4 for different values of laser power. From this Figure it can be seen that the ( $Rb^+$ ) shows a fast increase during the early stages of the interaction up to 5 ns followed by a linear increase up to 10 ns. Immediately after this time the density of  $Rb^+$  density shows a slow increase during the late stage of the irradiation time. This behaviour is due to the  $Rb^+$  mainly produced by the Penning ionization, photionization and laser-assisted Penning ionization processes as follows



Where nl states are populated in energy pooling collisions of two  $Rb(5p)$  atoms :

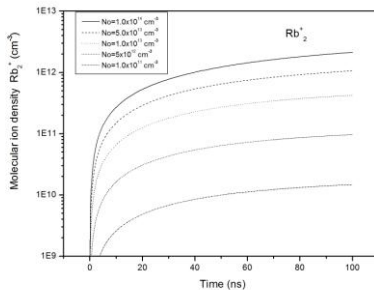


Figure.2. Time evolution of Molecular ion  $Rb_2^+$  at different rubidium vapour densities and laser power  $1 \times 10^5 \text{ W.cm}^{-2}$ .

### 3.2 The time evolution of the molecular ion $Rb_2^+$

The growth rate of the molecular ion  $Rb_2^+$  as a function of time is illustrated in Figure.2 for different values of laser power. From this Figure we can see that the  $Rb_2^+$  density shows a fast increase during the period 0.1 ns up to 5ns followed by a linear increase up to 20 ns. Immediately after this time the  $Rb_2^+$  density shows a slow increase during the late stages of the irradiation time. An understanding of this behaviour can be attained by considering that the main processes for producing these molecular ions are associative ionization(AI) and Hornbeck-Molnar ionization processes(MHI) as follows: $Rb(5p)+Rb(5p) \rightarrow Rb_2^++e (\epsilon_v)$  (AI)



where  $\epsilon_v$  is the kinetic energy of the free electrons emitted when  $Rb_2^+$  ion formed in the mean relative kinetic energy of the colliding atoms in the beam. Generally, the linear shape of  $Rb_2^+$  and the linear and quadratic term exchange show that the only possible mechanism for producing the molecular ion is (AI) at a certain density of Rb atomic vapour.

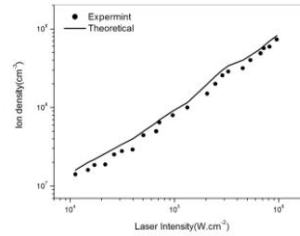


Fig.3. Variation of ion density of rubidium atoms with laser radiation intensity under excitation by nanosecond laser pulse to the resonant transition  $5S_{1/2} \rightarrow 5P_{3/2}$  at  $N_{Rb}=1.4 \times 10^{13} \text{ cm}^{-3}$ .

### 3.3 Variation of the ion density with the laser intensity

Figures 3 and 4 show relations of the ion density  $N_i$  versus laser intensity for the resonant transition  $5S_{1/2} \rightarrow 5P_{3/2}$  and  $5S_{1/2} \rightarrow 5P_{1/2}$  at rubidium vapour density namely;  $1.4 \times 10^{13} \text{ cm}^{-3}$  and  $4 \times 10^{13} \text{ cm}^{-3}$  respectively. From figure 3 it is clear that the behaviour of the calculated ion density agrees with those experimentally measured by Bakhrarov et al[10] during the initial stage of ionization (at low laser intensity= $1 \times 10^5 \text{ W.cm}^{-2}$ ), the results showed slopes 2 and 1.8 respectively.

This indicates that in figure 3 (the lower Rb density) the production of the seed electrons and formation of ion current proceeds mainly via two photon ionization process. This in turn increases the probability of another type of associative ionization process due to collision of atoms in these highly excited states with the resonantly excited atoms in the 5p state which is known as Hornbeck-Molnar ionization [4]. In addition to, atoms in highly excited states can appear in collisions between two resonantly excited atoms by laser radiation, where the excitation energy of one atom can be partially transferred to the other- energy pooling collision. Therefore, rubidium atoms in highly excited states may be produced through this process, rather than step-by-step excitation of atoms by electrons impact Barbier and Cheret [4,5].

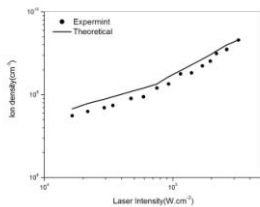


Fig.4. Variation of ion density of rubidium atoms with laser radiation intensity under excitation by nanosecond laser pulse to the resonant transition  $5S_{1/2} \rightarrow 5P_{1/2}$  at  $N_{\text{Rb}} = 4 \times 10^{13} \text{ cm}^{-3}$ .

On the other hand, for the resonance transition  $5S_{1/2} \rightarrow 5P_{1/2}$  the relation between the ion density and laser intensity are plotted for the atomic vapour density  $4 \times 10^{13} \text{ cm}^{-3}$  and shown in figure 4. It is noticed that the behaviour of the calculated ion density agrees reasonably with those measured ones over the examined range of the laser intensity. This again may be attributed to the various physical processes included in the model which depends on the population density of the highly excited states, where the ion density starts growing slowly followed by a faster rate as the laser intensity increases, the ion density increases linearly with the laser intensity. This linear behaviour assures the dominant contribution of the process of laser-assisted Penning ionization in providing the initial electrons required for plasma generation.

#### 4. Conclusions

A developed a model of dense rubidium vapor ionization induced by nanosecond resonant laser pulses exciting the  $5S \rightarrow 5P$  is applied to study kinetics of the processes which produce the molecular ion  $\text{Rb}_2^+$  and the atomic ion  $\text{Rb}^+$  was

investigated theoretically. The result of the model show that collisional ionization processes such as the associative ionization and Hornbeck-Molnar ionization play the important rule in producing the molecular ion density  $\text{Rb}_2^+$ . In addition to the competition between associative ionization (5P-5P), and Molnar-Hornbeck ionization processes for producing  $\text{Rb}_2^+$ , the calculations have also shown that the atomic ions  $\text{Rb}^+$  are formed through the Penning ionization and photoionization processes. These results are found to be consistent with the experimental observations. The good agreement shown in compare the calculated and measurement values of the formed  $\text{Rb}^+$  and  $\text{Rb}_2^+$  revealed the validity of the model in investigated the plasma generation using LIBORS technique.

#### References

- [1] A.N.Klyucharev, Physics-Uspekhi 36(6)(1993)486.
- [2] A.N.Klyucharev, N.N.Bezuglov, A.A.Matveev, A.A.Mihajlov, Lj.M.Ignjatovic and M.S.Dimitrijevic, New Astronomy Reviews 51 (2007)547.
- [3] T.B.Lucatoro and T.J.McIlrath, Appl. Opt. 19 (1980) 3948.
- [4] L.Barbier and M.Cheret, J. Phys. B: At. Mol. Phys., 16 (1983) 3213
- [5] L.Barbier and M.Cheret, J. Phys. B: At. Mol. Phys., 20(1987) 1229
- [6] M.Cheret and L.Barbier, L, J. Physique, 46(1985) C1-193.
- [7] D.Veza and C.J.Sansonetti, Z.Phys.D-Atoms, Molecules and Clusters 22(1992)463.
- [8] H.Skenderovic, I.Labazan, S.Milosevic, and G.Pichler, Phys.Rev A62,052707(2000)052707.
- [9] A.Kallenbach, and M.J.Kock, J.Phys.B22 (1989)1691.
- [10] S.A.Bakhramov, E.V.Vaganov, A.M.Kokhkharov and O.V.Parpiev, Proceeding of SPIE, Vol. 4748 (2002) 205.
- [11] M.A.Mahmoud, J. Phys. B: Atomic, Molecular & Optical physics, 38(2005)1545.
- [12] M.A.Mahmoud, A.M, Cent. Eur. J. Phys., 6(2008) 530.
- [13] W.H.Drawin, Rapport Euratom CEA. FC (1967) 383.
- [14] L.Vriens, J. Appl. Phys., 44(1973) 3980.
- [15] M. Aymar, E.Luc-Koenig, and F.Combet-Farnoux, J.Phys.B: At. Mol. Phys., 9(1976) 1279.
- [16] M.Aymar, O.Robaux and S.Wane, J. Phys. B: At.Mol.Phys., 17 (1984) 993.